Backbone model for confined masonry walls for performance-based seismic design

Zahra Riahi, Kenneth J. Elwood, and Sergio M. Alcocer

Abstract: In this study, a performance-based model is proposed capable of simulating seismic behavior of typical confined masonry (CM) walls whose response is governed by shear deformations. This model is developed on the basis of both monotonic and reversed-cyclic experiments assembled in an extensive database, and derived through an iterative linear regression analysis. Owing to the limited data available and inconsistencies in observed behavior in some tests, only specimens with two tie columns, one on either edge of the wall; multiple longitudinal rebar per confining element; no bed joint reinforcement; no openings within the confined panel; and a height- to- length ratio that varies from 0.7 to 1.2, are considered for the purpose of model development. The effect of openings on strength characteristics, the capability of existing models to predict seismic behavior of CM walls, and the limitations of the proposed equations are discussed in detail. The accuracy of the model is also verified for CM walls with different characteristics. The proposed model simulates reasonably well the seismic behavior of CM walls whose properties conform to the assumptions of the model and that correspond to typical CM walls.

Introduction

Confined masonry (CM) consists of load-bearing walls surrounded by small cast-in-place reinforced concrete tie columns and bond beams. CM is used as the lateral force resisting system for low-rise construction throughout the world; including Mexico, South and Central America, South-East Asia, Middle East, and South-Eastern Europe. The distinguishing feature of CM construction is that the masonry wall is constructed prior to the casting of tie columns and bond beams (see Figure 1a), forcing the wall and concrete elements to act as an integral unit when subjected to lateral loads. As illustrated in Figure 1b, in general, tie columns have a square section whose dimensions typically correspond to the wall thickness. For bond beams, however, both wall thickness and floor type influences the dimensions. Tie columns and bond beams are intended to confine the masonry panel, thus enhancing wall deformation capacity,

and connectivity with other walls and floor diaphragms. The in-plane response of a CM wall is distinctly different from that of a reinforced concrete frame with masonry infills, where the frame is constructed prior to the masonry infill. While CM wall experiences both flexural and shearing deformations, the masonry infill deforms in a shear mode within a frame that attempts to deform in flexure, resulting in separation of the frame and infill wall along the tension diagonal.

Performance-based seismic design relies on analytical models capable of simulating the performance of structures up to and including the lateral load strength degradation branch. Backbone response curves– which define the characteristic force-deformation relations from cracking to lateral load failure as a function of design parameters– must be developed and verified to enable the application of performance-based seismic design to CM structures. Typically, CM walls have been tested up to drifts corresponding to a 20% degradation of peak shear strength. For the purpose of this study, lateral load failure is defined at this deformation level.

Until now, complete backbone models have not been proposed for CM walls and past model development, summarized in Table 1, has focused only on cracking or maximum shear strength predictions. CM is not currently covered by the MSJC (MSJC 2008); and hence, MSJC capacity model has not been included in the table.

The performance of the existing models in predicting the load-carrying characteristics of Specimen 601 from Flores (2004), taken as a representative example of "typical" CM walls through this study, is compared in Figure 2 for a range of axial stress. As is evident from the graphs, cracking and maximum strength predictions vary considerably depending on the selected model. However, the intent of the shear strength model provided in the Mexican Code (*NTC04*) was to capture the cracking strength of the wall, thereby providing additional conservatism in the strength prediction (Meli, 1975). Similar approaches may have been adopted by other codes shown in Figure 2, partly explaining the wide range of predicted values for the maximum shear strength. In addition, typical masonry units, dimensions, and detailing of CM walls (e.g. tie columns) vary widely among countries, thus leading to somewhat different models.

As Table 1 shows, CM cracking shear strength is governed by panel characteristics, and tie column contribution is of significance only after cracking. However, only a few models (*MC06*, *AIJ99,* and *TK97*) rely on such tie column design variables as longitudinal reinforcement ratio, concrete compressive strength, and the number of tie columns in order to predict the maximum shear capacity of CM walls. Furthermore, the equations of this table are either influenced by the formulas originally developed for unreinforced (URM) and reinforced masonry (RM) panels or were developed based on a limited number of experiments (e.g. Tomazevic and Klemenc, 1997(a)). To be considered robust and indicative of the performance of CM walls with a broad range of design variables, accurate models should be calibrated to data from extensive databases such that analytical predictions match experimental results.

Deformation characteristics of CM walls, on the other hand, have only been addressed in a limited number of studies (Astroza and Schmidt, 2004; Urzua et al., 2001) which suggest empirical drift limits at different performance levels using experimental results. However, no current model can be relied on to predict the deformation response of CM walls on the basis of panel and confining elements characteristics.

The main objective of this study is to develop a backbone model for "typical" CM walls with the following characteristics:

- two tie columns, one on either edge of the wall;
- multiple longitudinal rebar per confining element;
- no bed joint reinforcement;
- no openings within the confined panel;
- height to length ratio that varies from 0.7 to 1.2.; and
- governed by shear deformations.

In order to assess the robustness of the proposed model, the effect of openings on the strength characteristics, and the validity of the predictive equations for specimens with bed joint reinforcement and high axial loads are investigated. Furthermore, the capability of existing models in simulating the seismic behavior of CM walls is also compared with the proposed model.

Limit states and model parameters

To develop the backbone model of this study, limit states (cracking, maximum strength, and ultimate deformation capacity) and their associated model parameters (variables that define the limit states) were identified and measured for individual tests on the basis of the recorded response.

To determine the model parameters first a smooth backbone was fitted to both positive and negative branches of the recorded response, by implementing the methodology recommended in ASCE/SEI 41 Supplement 1 (Elwood et al., 2007). This backbone (solid line in Figure 3.a) was drawn through the peak displacements of the first cycles at each deformation step. A trilinear backbone (dash line in Figure 3.a), was then fit to the smooth backbone for each individual test. This trilinear backbone that passes through the three defined limit states, was constructed considering the general aspects of seismic behavior of CM walls described below:

i) As previous studies suggest, for a typical CM wall, whose response is predominantly governed by shear deformations, the wall and its confining elements work monolithically at the early stages of loading, and the response is linear-elastic (Tomazovic and Klemenc, 1997(a), Zavala et al., 1998). However, the onset of inclined cracks and their extension towards tie columns reduce the stiffness of the panel. The point at which the first significant cracking occurs is accompanied by approximately 40% decline in the panel stiffness for the considered data. This point is chosen as the cracking point of the proposed model and is defined by two parameters: cracking shear stress (v_{cr}) and its associated drift ratio (δ_{cr}).

ii) Tie columns start to play a role after cracking limit state is reached. Dowel action of longitudinal reinforcement, which may be augmented by proper detailing of transverse reinforcement, friction, and brick interlock are the most significant contributors to the shear resistance of confining elements and masonry panel after cracking (Flores and Alcocer, 1996; Tomazevic and Klemenc, 1997(a)). As experimental results suggest, the maximum strength observed in the recorded response is reached when the diagonal cracks extend through tie column ends. This point represents the maximum

point of the backbone model, and is captured with two parameters; the maximum shear stress (v_{max}) and the associated drift ratio (δ_{max}).

iii) Concrete crushing, buckling/rupture of column longitudinal reinforcement, and masonry crushing are the most important factors giving rise to the strength and stiffness deterioration for CM walls (Alcocer, 1997; Ishibashi et al., 1992). As noted previously, the drift ratio at 20% strength loss from the maximum measured shear was chosen as the last model parameter of this study (δ_{ult}).

Existing models, results of previous studies, and fundamentals of CM structural behavior were all used in selecting the most effective CM design variables and to set the functional form of the model equations. Performing the regression analysis and investigating the existing trends between residuals (prediction errors) and design variables then assisted in improving the form of the preliminary equations.

The iterative regression analysis of this study was performed using the statistical software Stata (Stata 2007). In the process of model development those design variables whose contribution to the model were found to be insignificant were eliminated, without sacrificing model accuracy. For detailed information on the regression procedure the reader is referred to Riahi (2007).

Experimental database

A database of 102 CM walls was considered in the development of the empirical equations of this study. This database includes monotonic and reversed-cyclic static tests on cantilever and double-curvature CM walls. For a complete list of tests and their most important design variables and model parameters refer to Riahi (2007).

In an effort to focus on the behavior of "typical" CM walls, specimens with the following characteristics were not considered in the development of the models: more than two tie columns, openings in CM walls, simplified reinforcement detailing of tie columns (e.g. single longitudinal rebar and spiral hoops), and panel reinforcement. Specimens with the following characteristics were also omitted from the database:

- anomalies in recorded data.
- unspecified or unclear parameters.
- diagonal compression loading.
- interior tie columns, and no column transverse reinforcement.
- axial stress higher than $0.12f_m$. This limitation was imposed to avoid the occurrence of premature masonry crushing which according to previous studies may result in a significantly brittle failure mode (San Bartolome et al., 2004; Astroza and Schmidt, 2004).
- aspect ratio larger than 1.2. This limit was set due to the lack of sufficient data with aspect rations greater than 1.2 and the predominance of flexural deformations for CM walls with very large aspect ratios (approximately beyond 2.0).
- tie column reinforcement below 1%: This limitation was also imposed to avoid the predominance of a flexural failure mode.
- unusual testing procedure or complex geometry (e.g. 3D specimens).

Considering all mentioned constraints, the ranges of all important CM variables are listed in Table 2.

Owing to the lack of information on some design variables and model parameters, each model equation, however, was developed on the basis of a subcategory of the considered database. The number of data points included in the evaluation of v_{cr}, v_{max}, δ_{cr}, δ_{max}, *and* δ_{ult} were 80, 39, 42, 37, and 38, respectively.

Proposed model for cracking shear strength (v_{cr})

Equation development

On the basis of existing models, visual trends, and formulation of the linear elastic behavior (idealizing masonry panel as a cantilever shear beam for squat walls), significant design variables were selected and formulated into a suitable functional form. Running the regression analysis though an iterative process, data inspection after each iteration, and checking the fitness of the model and its overall significance, then resulted in establishment of the final form of Equation 1.

$$v_{cr} = Min\left(0.424 \cdot v_m + 0.374 \cdot \sigma_v,\ v_m\right) \qquad \textbf{(Equation 1)}$$

Cracking shear capacity of CM walls in Equation 1 is limited to the masonry shear strength, v_m. As is apparent from this equation, v_{cr} is governed by panel characteristics, and tie column contribution in the linear-elastic range is not significant. Furthermore, statistical measures suggest that v_m and σ_v contribute equally to Equation 1, and therefore both masonry shear strength and axial load are of importance to the cracking shear strength of CM walls. As is shown in Figure 4, the proposed model predicts CM cracking shear strength with acceptable accuracy. Also shown in the graph are dashed lines corresponding to +/- one standard deviation.

Comparison with existing models

The form and constituent variables of the proposed equation to predict v_{cr} are similar to the existing cracking models (Table 1). However, neither *M88* that greatly overestimates the shear cracking strength of CM walls, nor *CC97* and *MAT94* that are over-conservative, are appropriate for design purposes (see Table 3).

Since four of the seven existing models for maximum shear strength rely only on panel characteristics, they are also compared with Equation 1 to identify how well they predict the cracking shear strength (Table 3). *NTC04*, *CC93* and *PC98* match both the experimental data and the proposed equation. However, *AC83* with much higher v_m coefficient, and *AIJ99*, *MC06*, and *TC07* which incorporate the contribution of tie columns in their equations fail to properly predict v_{cr}. As noted earlier, *NTC04* ignores the influence of tie columns since the maximum shear strength is conservatively approximated by the cracking strength; hence, as expected, this model provides a better estimate of the cracking strength than the maximum shear strength.

The effect of openings

Openings are believed to adversely affect the seismic performance of CM walls, and therefore, their size, location, and number in addition to their confinement detailing, have recently received considerable attention (Ishibashi et al., 1992; Yañez, et al., 2004; and Flores et al., 2004). Keeping the size of openings as the only varying factor

between typical CM walls, 14 specimens tested by Yañez et al. (2004) were used for the assessment of opening effects on v_{cr}.

To identify the effect of openings, a plot of v_{cr} versus β (the ratio of the opening area to $H_w L_w$) was drawn and a linear relationship was fitted to the experimental data. As Figure 5 shows, an increase in the opening size results in a relatively sharp decline in the cracking shear strength of the solid specimen with the same characteristics (i.e. $\beta=0$). Since it was developed only for 14 specimens, Equation 2 should be use with caution.

$$v_{cr}(\beta \neq 0) = (-2.2 \cdot \beta + 1) \cdot v_{cr\ eqn1} \qquad \textbf{(Equation 2)}$$

Proposed model for maximum shear strength (v_{max})

Equation development

Database results suggest that the maximum shear strength is, on average, 1.3 times the cracking strength of the panels, implying the post-cracking contribution of tie columns and the confinement they provide to be of significance for the seismic performance of CM walls. As a result, panel characteristics (H_w/L_w, v_m, and σ_v) and tie column design variables ($\rho_{vc}.f_{yvc}$, $\rho_{hc}.f_{yhc}$, and f'_c) along with the type of masonry units were considered in the prediction of maximum shear strength of CM walls. From the regression analyses, it was found that unit type, panel aspect ratio (H_w/L_w), and tie column transverse reinforcement were insignificant and thus were excluded from Equation 3.

$$v_{max} = 0.21 \cdot v_m + 0.363 \cdot \sigma_v + 0.0141 \cdot \sqrt{\rho_{vc} \cdot f_{yvc} \cdot f'_c} \geq v_{cr} \qquad \textbf{(Equation 3)}$$

No specific trend with transverse reinforcement is evident from Figure 6, used to illustrate the ability of the proposed model to predict the maximum shear strength of CM walls, thus supporting the exclusion of transverse reinforcement from Equation 3.

Based on statistical measures, axial stress is the most significant variable in this equation, followed by the term that accounts for the contribution of tie columns. At this stage of response, the contribution of masonry shear strength, v_m, is minimal compared to other variables.

Comparison with existing equations

As shown in Table 3*, MC06*, *AIJ99, and TK97*– the only models that consider tie column design variables– fail to closely match the experimental results. In spite of being very similar in its formulation to the empirical model of this study, *TK97* overestimates the contribution of tie columns by over three times. This may be attributed to the development of this model on the basis of a limited number of tests that were removed from the database used for the current study, since unique similitude laws were used to scale the specimens, and hence, were not comparable to the rest of the database.

Despite not considering tie column design variables, *AC83*, on average, provides a good estimate of v_{max} (see Table 3). However, accentuating the contribution of panel shear strength, which is not as significant as other variables at this stage, may be considered a weakness of *AC83*. It would be preferred to incorporate the effect of tie columns in the axial stress term, if simplicity were the goal.

Proposed model for cracking drift capacity (δ_{cr})

Idealization of typical CM walls as cantilever shear beams, and assuming a linear relationship between cracking shear capacity and its corresponding drift ratio assisted the formulation of cracking drift capacity equation, for which no previous model existed.

Assuming masonry as approximately homogeneous prior to cracking, its shear modulus may be related to its elastic modulus; the latter, however, is typically proportioned to the masonry compressive strength in masonry codes. As a result, f_m was initially selected as a representative of the masonry shear modulus, and v_{cr} (from Equation 1), composed of three independent variables itself, was chosen as the second contributing design variable. The presence of a clear trend in the plot of residuals versus the predictor variable after the first regression analysis, however, resulted in a square root transformation for f_m. The type of unit materials, also proved significant, and was therefore included in the final formulation of the model. Due to the lack of sufficient data on CM walls with ceramic units, however, these units were excluded from equation 4.

$$\delta_{cr} = \gamma \cdot \frac{v_{cr\ eqn1}}{\sqrt{f_m}} \quad , \qquad \gamma = \begin{pmatrix} 1.13 & \text{,clay} \\ 0.72 & \text{,concrete} \end{pmatrix} \qquad \textbf{(Equation 4)}$$

In this equation v_{cr} and f_m are in MPa units.

Concrete units, in general, are more brittle than clay bricks, and have a smaller gamma value as a result in Equation 4.

Proposed model for ultimate drift capacity (δ_{ult})

Lack of existing models for the ultimate deformation capacity of CM walls, nonlinearity of the response, and contribution of both panel and tie column design variables to δ_{ult}, made variable selection and model specification extremely difficult at the ultimate limit state. However, shear strength degradation, as noted previously, may be mainly ascribed to concrete and masonry crushing, and rebar rupture/buckling. As a result, tie column concrete compressive strength (f'_c), tie column longitudinal and transverse reinforcement ($\rho_{vc}.f_{yvc}$, $\rho_{hc}.f_{yhc}$), the ratio of the hoop spacing to tie column width (s/w_{tc}) and axial stress to masonry compressive strength ratio (σ_v/f_m) were initially considered as significant variables. The dependence of stiffness degradation on unit materials and unit geometry (i.e. hollow or solid) also resulted in the inclusion of these variables in the model. Masonry units with net area larger than 0.75 times the gross area were considered solid for the purpose of this study.

The yield drift ratio of an equivalent system (δ_y) defined by pre-cracked stiffness and maximum shear capacity (Figure 3.b) was multiplied by a ductility factor (μ) to determine the ultimate drift capacity of CM walls. In fact, δ_y was first determined by substituting $v_{max\ eqn3}$ for $v_{cr\ eqn1}$ in Equation 4. All that remained therefore was to determine μ.

Selecting v_{max} from Equation 3 (reflecting the influence of v_m, σ_v, $\rho_{vc}.f_{yvc}$ and f'_c), and including unit material in the δ_y equation, transverse reinforcement ratio and the ratio of the hoop spacing to column width remained the only variables to be investigated. These variables, however, appeared insignificant to the model. No clear trend, for example, is evident between the measured ductility factor and $\rho_{vc}.f_{yvc}$ from Figure 7

even after separating the data into groups with the same characteristics. Therefore, column transverse reinforcement was excluded from the final model (Equation 5). As is clear from Equation 5b and Figure 8, a strong inverse relationship exists between the ductility factor and maximum shear strength of CM walls.

$$\delta_{ult} = \mu \cdot \gamma \cdot \frac{v_{max\ eqn3}}{\sqrt{f_m}} \qquad \textbf{(Equation 5a)}$$

$$\mu = \frac{0.5}{v_{max\ eqn3}^{2}} + 1.3 \leq 6 \qquad \textbf{(Equation 5b)}$$

Equation 5 was developed for walls with hollow/solid clay and hollow concrete masonry units. The value of μ for solid clay and hollow concrete units seems reasonable. However, as is evident from Figure 8, some walls with hollow clay units, contrary to the expected behavior, exhibit a very ductile behavior. The discrepancy may be related to the lack of sufficient data on typical CM walls made of these masonry units. As a result, the model should be used with caution for CM walls with hollow clay units and the calculated value of μ is recommended to be limited to less than 6. Ductility demands larger than 6 would result in excessively large diagonal cracks in CM walls and this may impact the integrity of the panel.

Despite inclusion of all potentially important variables, the presence of a constant in the ductility equation which is statistically significant, may be taken as an indicator of unknown variables that are contributing to the response. This constant may also be interpreted as implying that typical CM walls, regardless of the reinforcement detailing of tie columns and the type of masonry units, have an intrinsic ductility of approximately 1.8. Further research is required to assess the contribution of other design variables and the minimum ductility achieved by CM walls.

Proposed model for drift capacity at maximum strength limit state (δ_{max})

The limit state defined by δ_{max} and v_{max} is intended to capture the point at which the maximum strength occurs. However, rapid changes in deformation with limited increase in strength after cracking and yielding of a CM wall make it difficult to determine the drift ratio at maximum strength with acceptable accuracy ($\delta_{max}/\delta_{ult}$ from

the database ranges from 0.25 to 1.00). As a result, in Equation 6, δ_{max} is predicted simply as a fraction of the ultimate drift capacity, $\delta_{ult\ eqn\ 5}$.

$$\delta_{max} = 0.65\ \delta_{ult\ eqn\ 5} \qquad \textbf{(Equation 6)}$$

Since tighter limits might be sought in practice, the lognormal distribution of $\delta_{max}/\delta_{ult}$ is shown in Figure 9, in order to facilitate determination of this ratio at any desirable confidence level.

Comparison of drift models with existing empirical limits

Code provisions and past CM studies address the deformation capacity of CM walls only through recommended limits. Such limits, however, are not a function of CM design variables, thereby making a direct comparison between the proposed drift models and past CM research difficult. As a result, Table 4 only compares the database measured drifts from this study with the empirical limits of previous studies. As is shown in the table, the average measured drifts are comparable with results of past research. The allowable inelastic drift of the Mexican code (*NTC04)* in Table 4 is considerably lower than the average drift capacity of typical CM walls. However, this limit is intended to prevent CM walls from reaching drift ratios close to δ_{max} after which severe strength and stiffness degradations is likely to occur.

Discussion

Summary of the proposed equations

The empirical equations, 1, 3, 4, 5, and 6, are presented for all model parameters characterizing three different limit states: cracking, maximum strength, and ultimate deformation capacity. These predictive equations are proposed on the basis of the important tie column and panel characteristics of typical CM walls, and are developed through an iterative linear regression analysis. The most important design variables included in the model are: σ_v, H_w/L_w, f_m, v_m, $\rho_{vc}.f_{yvc}$, f'_c, and masonry unit type. Table 5 summarizes the mean, median, coefficient of variation, the number of data points included in the development of the equation for each model parameter (*N)*, and the coefficient of determination (R^2).

The lognormal fragility curves of experimental to calculated model parameters are presented in Figure 10 to further depict the variability of the proposed model. Such curves are also useful in practice where higher margins of safety might be sought. As is evident from these graphs, the model parameters are suffering from high variability which should be lowered through collection of more suitable data and the subsequent improvement of the model.

These fragility curves are also shown in Figure 11 for specimen 601 from Flores (2004) that fits in all the constraints of the proposed model (σ_v =0.55 MPa, H_w/L_w=0.97, f_m=5.25 MPa, v_m=0.42 MPa, f'_c=23.10 MPa, $\rho_{vc}.f_{yvc}$=4.29 MPa, and Unit type = concrete). The curves of Figure 11 constructed on the basis of fragility curves of Figure 10 and the proposed equations, may be used for determination of model parameters at any confidence level. For example, model parameters at 10% probability of failure for this wall are v_{cr}= 0.28 MPa, δ_{cr}= 0.1%, v_{max}= 0.33 MPa, δ_{max}= 0.14%, δ_{ult} = 0.33%, respectively.

Limitations of the analytical model

The primary limitation of the proposed model is that all empirical equations are derived for CM walls whose response is governed by shear deformations. In general, any violation from this major assumption– predominance of shear deformations– could disturb the accuracy of the model. The applicability of these predictive equations is also limited by being developed only for "typical" CM walls. That is, the developed model best simulates the seismic performance of:

- panels with identical reinforcement detailing for both tie columns
- CM walls with sufficient tie column longitudinal reinforcement whose response is not dominated by either premature rebar yielding or crushing of the masonry. The database results suggest that the desired behavior is observed if the tie column longitudinal reinforcement ratio falls between 1% and 3%.
- CM walls with panel aspect ratios (H_w/L_w) less than or equal to 1.2.
- panels with axial stress (σ_v) less than $0.12f_m$ such that the response is not controlled by premature masonry crushing.

The applicability of the derived equations is also limited by the range of design variables included in the development of the model, particularly after removal of data with extreme values on single or multiple design variables (Table 2).

Approximately 80% of the specimens considered in developing the backbone model were tested using reversed cyclic loading protocol. However, this loading method with 2-3 cycles per deformation level may not be consistent with earthquake loading that typically results in a few cycles with large deformations before the ultimate limit state. In addition, it should be kept in mind that the empirical equations are developed on the basis of laboratory tests with highly controlled construction and material qualities. Actual CM walls, however, are likely to have lower capacities, especially since material properties and workmanship are highlighted as key factors substantially affecting the seismic performance of CM walls (Alcocer et al., 2003).

The application of performance-based seismic design principles in masonry structures is moving forward very slowly. Thus, the model developed provides a robust tool for designers and code-developers to assess the adequacy of current design procedures, as well as, and quite importantly, to implement design requirements based on engineering techniques, instead of the historical rules-of-thumb that have characterized this construction system.

Evaluation of the proposed equations

Due to the inclusion of all the available data in the development of the empirical equations, evaluation of the model by selecting suitable data from outside the sample space was not possible in this study. As a result, database specimens with a complete set of model parameters were considered for the purpose of model evaluation.

Previous CM models and test experiments have been developed independently across the globe for understanding the behavior of CM walls constructed as per local practice and available materials, and were not aimed for development of a “universal” model.

However, as Figure 12 illustrates, keeping each design variable within its practical range, the empirical backbone model of this study is capable of predicting the recorded response with sufficient accuracy, stressing the fact that such universal trends exist for typical CM walls.

Figure 13 shows the response curves for a specimen with σ_v/f_m equal to 0.14. The occurrence of premature masonry crushing limits the deformation capacity of this specimen, and the model over-predicts the ultimate drift capacity by almost 25%.

The backbone response of Specimen M-1/4-E6 from Aguilar et al. (1996), as a representative of CM walls with bed joint reinforcement (ρ_{hw} = 0.18%), is shown in Figure 14 in order to evaluate the accuracy of the model for this group of atypical CM walls. Proposed equations adequately predict the model parameters at cracking limit state which is believed to be independent of reinforcement detailing of the panel and confining elements (Yoshimura et al., 2004; Hernandez and Meli, 1976; Aguilar et al., 1996). However, the response at both maximum and ultimate limit states is under-predicted by the empirical equations, due to the beneficial effects of horizontal reinforcement on both deformation and strength characteristics of the panels.

As a result, the model predicts reasonably well the seismic response of CM walls that fit the constraints of the proposed equations, but fails to track the response curves of atypical or anomalous specimens.

Conclusions and Recommendations

The proposed backbone of this study is developed on the basis of the panel and tie column characteristics of 102 monotonic and reversed-cyclic experiments, and is proposed for typical CM walls with aspect ratios less than or equal to 1.2. The equations which characterize three different limit states -cracking, maximum strength, and ultimate deformation capacity- are deterministic in nature and are intended to capture the average response from the database. Model uncertainties are represented by fragility curves. The seismic response of the specimens that fit the constraints of the model is predicted by these empirical equations with sufficient accuracy. However, the proposed model fails to match closely the recorded response of atypical CM walls (e.g. aspect ratios above 1.2, tie columns with one longitudinal bar, axial stress greater than $0.12f_m$, etc.). As a result, future testing should be conducted, either to relax some of the currently imposed limitations that stem from the lack of data, or to assess the effects of other contributing factors. CM walls with openings, panel reinforcement, multiple confining elements, or high axial stress are among the categories that should be included in future CM wall tests.

Tie column transverse reinforcement is one of the design variables that proved insignificant to the ultimate deformation equation of this study. However, due to the presence of a large constant in the proposed equation which is also statistically significant, and considering the crucial role that transverse reinforcement is believed to have in confining the core concrete and augmenting the dowel action of longitudinal reinforcement, it is highly recommended this factor be studied more closely in future research on the topic.

Current CM codes, as the basis of design and construction, mainly rely on conventional force-based equations that were originally developed for URM/RM walls, and the effect of confining elements has been overlooked by many of the code equations. As a result, such models are incapable of predicting the recorded response with sufficient accuracy. In addition, deformation characteristics of CM walls, that are believed to be more closely correlated with sustained earthquake damage, are rarely reflected in masonry codes. The allowable drift limit stipulated in the Mexican code is found to be conservative compared to the measured response of the walls included in the database. The outcome of this research, however, could contribute to the development of more accurate models and guidelines for improvement of these currently deficient provisions.

Acknowledgements

Support for the research presented in this paper was provided by the Earthquake Engineering Research Institute and the Natural Sciences and Engineering Reasearch Council of Canada. This support is gratefully acknowledged.

Notation

The following symbols are used in this paper:

A_{hc}	=	tie column transverse reinforcement area
A_{stc}	=	cross sectional area of tie column longitudinal reinforcement in AIJ model (1999)
A_{tc}	=	tie column cross-sectional area
A_{vc}	=	tie column longitudinal reinforcement area

A_w	=	wall cross-sectional area including tie columns
D	=	Distance between centroids of tie columns in Matsumura's model
d_b	=	Diameter of longitudinal bar in Tomazevic and Klemenc's model
f'_c	=	concrete compressive strength
f_m	=	masonry compressive strength
f_{yhc}	=	yield strength of column transverse reinforcement
f_{yvc}	=	yield strength of column longitudinal reinforcement
f_{yhw}	=	yielding strength of panel horizontal reinforcement
H_w	=	wall height
J	=	Internal lever arm under bending in Matsumura's model
k_u	=	reduction factor for Matsumura's model
L_w	=	wall length including tie columns
N	=	number of observations (Table 5)
N	=	number of tie columns in Marinilli and Castilla model (2006)
N	=	Number of longitudinal bar in tie column in Tomazevic and Klemenc's model (1997)
N_{tc}	=	number of tie columns
S	=	vertical spacing between tie column transverse reinforcement
v_m	=	masonry shear strength from diagonal compression tests
v_{cr}	=	cracking shear stress
v_{max}	=	maximum shear stress
w_{tc}	=	tie column width
A	=	the effect of panel aspect ratio on panel resistance
β	=	the ratio of the opening area to the wall gross area, $H_w L_w$
γ	=	the effect of unit material on the panel rigidity
δ_{cr}	=	cracking drift capacity (fraction of wall height)
δ_{max}	=	drift capacity at maximum limit state(fraction of wall height)
δ_{ult}	=	ultimate drift capacity (fraction of wall height)
δ_y	=	drift capacity of the equivalent linear system (fraction of wall height)
M	=	ductility factor (δ_{ult}/δ_y)

ρ_{hc} = tie column transverse reinforcement ratio ($A_{hc}/(t_{tc}.\ s)$)

ρ_{vc} = tie column longitudinal reinforcement ratio (A_{vc}/A_{tc})

σ_v = axial stress (based on wall overall area A_w)

References

Aguilar, G., Meli, R., Diaz, R., and Vazquez-del-Mercado, R., (1996). "Influence of Horizontal Reinforcement on the Behavior of Confined Masonry Walls," Proceedings, 11th World Conference on Earthquake Engineering, Acapulco, Mexico, No. 1380.

AIJ, (1999). Architectural Institute of Japan (AIJ) Committee for Concrete and Masonry Wall Building Structures (1999),"Ultimate Strength and Deformation Capacity of Buildings in Seismic Design." 592-593.

Alcocer S.M. (1997). "Comportamiento sísmico de estructuras de mampostería: una revisión," State of the Art paper, Proceedings, XI Congreso Nacional de Ingeniería Sísmica, Veracruz, México, 164-191.

Alcocer S.M., Cesín J., Flores L.E., Hernández O., Meli R., Tena A., y Vasconcelos D. (2003). "The New México City Code Requirements for Design and Construction of Masonry Structures," Memorias de la Ninth North American Masonry Conference, ISBN 1-929081-16-2, Clemson, South Carolina, EUA, pp. 656-667

Alcocer S.M. and Meli R. (1995). "Test Program on the Seismic Behavior of Confined Masonry Structures," The Masonry Society Journal, The Masonry Society, vol. 13, no. 2, USA, pp. 68-76.

Astroza M.I., and Schmidt A.A. (2004). "Capacidad de deformación de muros de albañilería confinada para distintos viveles de desempeño (Deformation capacity of confined masonry for different performance levels)." Revista de Ingeniería Sísmica, 70, 59-75

Elwood K.J., Matamoros A.B., Wallace J.W., Lehman D.E., Heintz J.A., Mitchell A.D., Moore M.A., Valley M.T., Lowes L.N., Comartin C.D., and Moehle J.P.(2007) "Update to ASCE/SEI 41 concrete provisions." Earthquake Spectra

Flores, L. E., and Alcocer, S. M. (1996) "Calculated response of confined masonry structures." 11th World Conference on Earthquake Engineering, Acapulco, Mexico, Paper No. 1830

Flores, L.E., Mendoza, J.A., and Reyes, C., (2004) "Ensaye de Muros de Mampostería con y sin Refuerzo Alrededor de la Abertura," (in Spanish), Proceedings, XIV National Congress on Structural Engineering, , Acapulco, Mexico.

INN (1997)" Norma Chilena NCh2123.Of 97 (1997) Albanileria confinada-requisitos de deseno y calculo." Instituto nacional de normalizacion, Santiago, Chile

Inpres-Cirsoc 103. (1983) "Normas Argentinas para construcciones sismorresistentes". Parte III.Construcciones de Mampostería

Ishibashi, K., Meli, R., Alcocer, S.M., Leon, F., and Sanchez, T.A. (1992) "Experimental study on earthquake-resistant design of confined masonry structures." Proceedings of the Tenth World Conference on Earthquake Engineering, Madrid, Spain, 3469-3474

Marinilli, A., and Castilla, E. (2006) "Seismic behavior of confined masonry walls with intermediate confining - columns." Proceedings of the 8th U.S. National Conference on Earthquake Engineering, San Francisco, California, USA, No. 607

Matsumura, A. (1988) "Shear Strength of Reinforced Masonry Walls," Proceedings of the 9th World Conference on Earthquake Engineering, Tokyo-Kyoto, Japan, 121-126.

Meli, R. (1975). "Comportamiento Sísmico de Muros de Mampostería," Report No. 352, Instituto de Ingeniería, UNAM, Mexico City, 114 pp.

Moroni, M.O., Astroza, M., and Tavonatti, S., (1994)."Nonlinear models for shear failure in confined masonry walls." The Masonry Society Journal. Vol. 12, No. 2, 72-78

Norma Peruana de Diseño Sismorresistente E-070 (1998), Capítulo Peruano del ACI.

NTC-M (2004) "Normas tecnicas complementarias para diseno y construccion de estructuras de mamposteria" Gobierno del distrito federal

Riahi, Z. (2007)" Performance-based seismic models for confined masonry walls." Master thesis, University of British Columbia.

San Bartolome, A., Quiun, D., and Mayorca, P. (2004) "Proposal of standard for seismic design of confined masonry buildings." Bulletin of ERS, No. 37

Stata (2007)"Based reference manual." Stata press.

Tomazevic, M., and Klemenc, I. (1997a). "Seismic behavior of confined masonry walls." Earthquake engineering and structural dynamics, Vol. 26, 1059-1071

Tomazevic, M., and Klemenc, I. (1997b)."Verification of seismic resistance of confined masonry buildings." Earthquake engineering and structural dynamics, Vol. 26, 1073-1088

Urzua, D.A., Padilla, R., and Loza, R. (2001)" Influencia de la carga vertical en la resistencia síismica de muros de albañilería confinada elaborados con materiales pumíticos de Guadalajara"

Yañez, F., Astroza, M., Holmberg, A., and Ogaz, O.(2004)"Behavior of confined masonry shear walls with large openings" 13th World Conference on Earthquake Engineering, Vancouver, B.C., Canada, No. 3438

Zavala, T., Cabrejos R.T,and Tapia, J.G (1998)." Aseismic Masonry Building Model for Urban Areas" Structural Engineering World Wide, T209-1

Table 1: Existing models for cracking and maximum shear strength of CM walls

ID	Equations	Remarks	References
$V_{cr\text{-}M88}$	$Vcr = \left(\frac{k_u}{\frac{h_o}{d} + 2} \cdot \sqrt{f_m} + 0.3 \cdot \sigma_v \right) \cdot t_w \cdot j \cdot 10^3$ (N, mm)	k_u : reduction factor =0.64 for partially grouted walls and 1.0 for other walls. h_o j : 7/8 d, $d = L_w - W_{tc}/2$	Matsumura , 1988
$V_{cr\text{-}CC97}$	$V_{cr} = Min\left(0.23 \cdot v_m + 0.12 \cdot \sigma_v, 0.35 v_m\right) \cdot A_w$	——	Nch 2123, 1997
$V_{cr\text{-}MAT94}$	$V_{cr} = \left(0.19 \cdot v_m + 0.12 \cdot \sigma_v\right) \cdot A_w$	——	Moroni et al., 1994
$V_{max\text{-}NTC04}$	$V_{max} = Min\left(0.5 \cdot v_m + 0.3 \cdot \sigma_v, v_m\right) \cdot A_w$	——	NTC-M, 2004
$V_{max\text{-}CC93}$	$V_{max} = Min\left(0.45 \cdot v_m + 0.3 \cdot \sigma_v, 1.5 v_m\right) \cdot A_w$	——	Nch 2123, 1993
$V_{max\text{-}AIJ99}$	$V_{max} = \left[K_u \cdot K_p \cdot \left(\frac{0.76}{\frac{h_o}{d} + 0.7} + 0.012 \right) \cdot \sqrt{f_m} + 0.2\sigma_v \right] \cdot t_w \cdot j \cdot 10^3$ (N, mm)	k_u : the same as $V_{cr\text{-}M88}$ $k_p = 1.16 . \rho_t^{0.3}$ $\rho_t = A_{stc} / t_w . d$ $A_{s\,tc}$: cross sectional area of column longitudinal reinforcement	AIJ, 1999
$V_{max\text{-}PC98}$	$V_{max} = \left(0.5 \cdot \alpha \cdot v_m + 0.23 \cdot \sigma_v\right) \cdot A_w$	$\alpha = \frac{H}{L}, \frac{1}{3} \le \alpha \le 1$	E-070, 1998
$V_{max\text{-}MC06}$	$V_{max} = \left(0.47 \cdot v_m + 0.29 \cdot \sigma_v\right) \cdot \left(A_w - N \cdot A_{tc}\right) + 4200N$ (kg, cm)	N : number of tie columns	Marinilli and Castilla, 2006
$V_{max\text{-}AC83}$	$V_{max} = \left(0.6 \cdot v_m + 0.3 \cdot \sigma_v\right) \cdot A_w$	——	Inpres Cirsoc, 1983
$V_{max\text{-}TK97}$	$V_{max} = V_{cr} + 0.806 n \cdot d_b^2 \cdot \sqrt{f_c \cdot f_{yvc}}$ (N, mm)	d_b: Longitudinal reinforcement diameter n: number of longitudinal rebar	Tomazevic and Klemenc, 1997

Table 2: Ranges of important design variables for CM wall tests used in the development of the proposed model

Design Variable	Practical Range	Remarks
v_m	0.25 – 1.1 MPa	—
f_m	2.5 – 25 MPa	—
σ_v	0 –1 MPa	—
σ_v / f_m	0 – 0.12	—
f'_c	10 – 35 MPa	—
$\rho_{vc}. f_{yvc}$	2 – 15 MPa	—
ρ_{vc} (%)	1–3	—
ρ_{hc} (%)	0–0.8	—
H / L	≤ 1.2	—
Unit type	Clay, and Concrete	Due to the lack of data on ceramic units δ_{ult} is predicted only for concrete and clay units. The predictive equation should also be utilized with caution for hollow clay units.

Table 3: Comparison between existing models and observed cracking and maximum strength from database

Notations	$v_{cr(exp)} / v_{cr\ (cal)}$ *	$v_{\ max(exp)} / v_{max\ (cal)}$ *	References
$V_{cr\text{-}proposed}$	1.05 ± 0.25	—	—
$V_{cr\text{-}M88}$	0.51 ± 0.18	—	Matsumura, 1988
$V_{cr\text{-}CC97}$	2.24 ± 0.64	—	Nch2123, 1997
$V_{cr\text{-}MAT94}$	2.52 ± 0.62	—	Moroni et.al, 1994
$V_{max\text{-}proposed}$	—	1.00 ± 0.22	—
$V_{max\text{-}NTC04}$	0.97 ± 0.24	1.39 ± 0.38	NTC-M, 2004
$V_{max\text{-}CC93}$	1.05 ± 0.26	1.27 ± 0.35	Nch2123, 1993
$V_{max\text{-}AIJ99}$	—	0.96 ± 0.39	AIJ,1999
$V_{max\text{-}PC98}$	1.01 ± 0.26	1.29 ± 0.36	E-070, 1998
$V_{max\text{-}MC06}$	—	0.75 ± 0.21	Marinilli and Castilla, 2006
$V_{max\text{-}AC83}$	0.83 ± 0.21	0.97 ± 0.28	Inspres Cirsoc, 1983
$V_{max\text{-}TK97}$	—	0.69 ± 0.31	Tomazevic and Klemenc, 1997

* mean ± one standard deviation

Table 4: Comparison between the measured drifts and existing limits

ID	***Unit material***	δ_{cr}***(%)***	δ_{max}***(%)***	δ_{ult}***(%)***	***Reference***
–	Clay	0.122±0.051	0.455±0.290	0.765±0.310	Present study*
	Concrete	0.111±0.039	0.382± 0.192	0.586±0.176	
AS04	Ceramic and Concrete	0.130	0.400	0.730	Astroza and Schmidt, 2004
U01	Pumice	–	0.410	0.690	Urzua et al., 2001
NTC04	All	0.15	0.250 (allowable drift)		NTC-M, 2004

* mean ± one standard deviation given for measured drifts from database.

Table 5: Statistical characteristics of the proposed equations

Model Parameter	Unit Type	Mean (exp/cal)	Median (exp/cal)	COV (exp/cal)	N	R^2	Eqn No
v_{cr}	All	1.046	1.067	0.245	80	0.958	1
v_{max}	All	1.001	0.976	0.223	39	0.960	3
δ_{cr}	Clay	1.240	1.249	0.553	18	0.811	4
	Concrete	1.065	1.148	0.303	23	0.887	
δ_{max}	All	1.015	1.003	0.237	37	0.701	6
δ_{ult}	Clay	1.036	1.040	0.329	27	0.801*	5
	Concrete	0.937	0.961	0.189	11		

* Based on results shown in Figure 8, one ductility model is developed for all unit types.

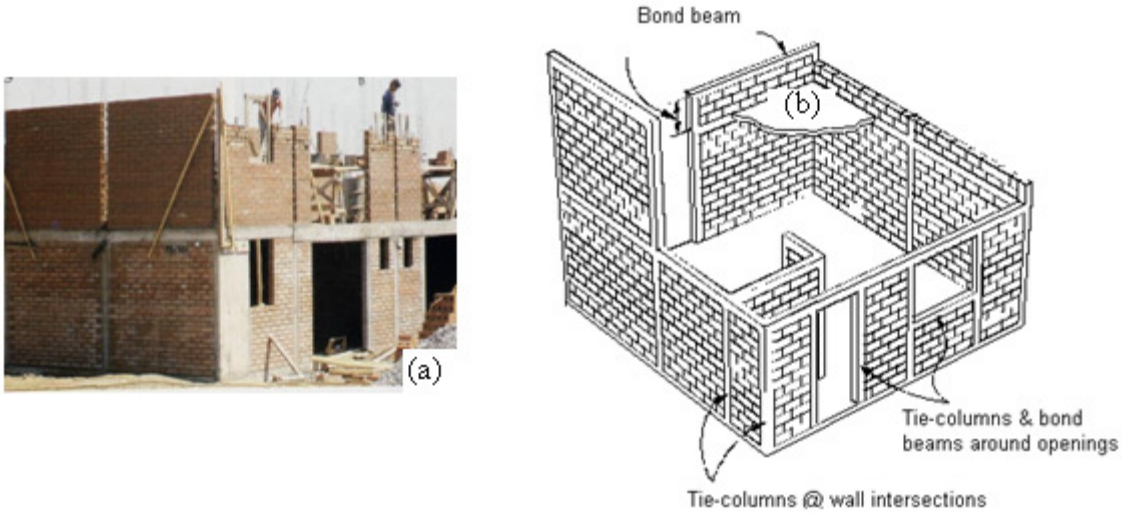

Figure 1:(a) Confined masonry wall under construction and, (b) primary components of confined masonry buildings.

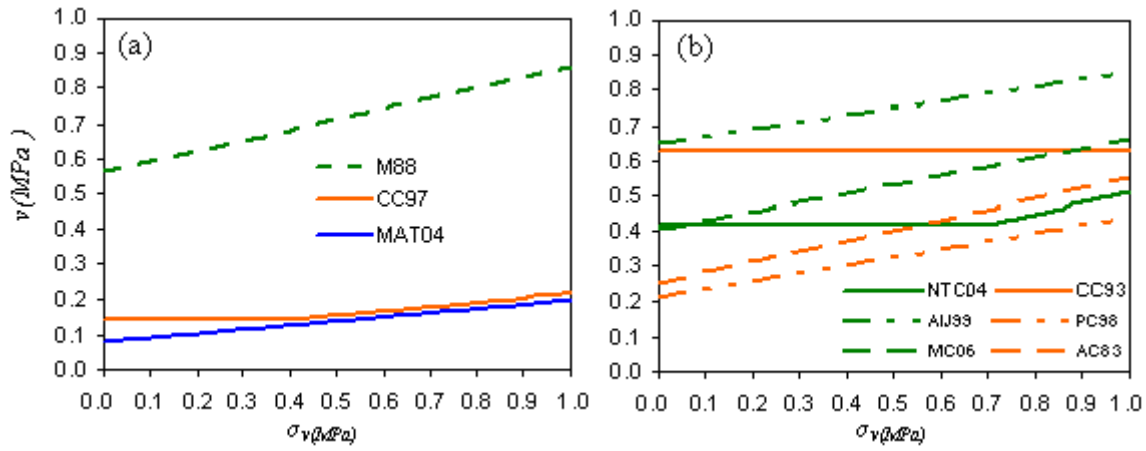

Figure 2: Comparison between the performance of existing models for Specimen 601 from Flores (2004) (a) Cracking shear strength, (b) Maximum shear strength

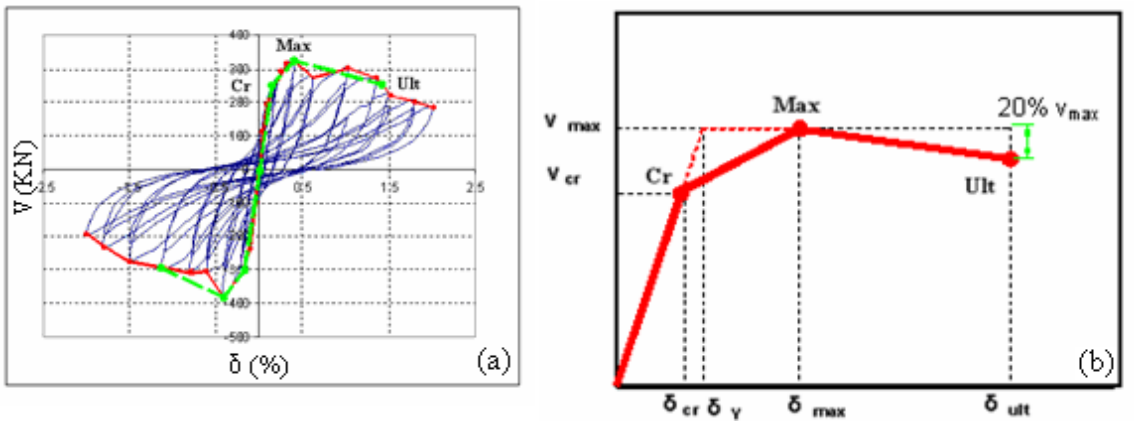

Figure 3: (a) Example of determination of model parameters on the basis of the recorded response (Specimen M-147, Ishibashi et al., 1992), (b) Backbone model of the current study

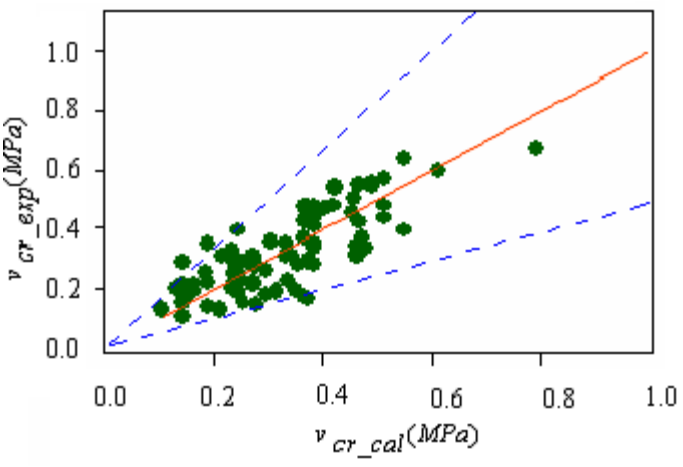

Figure 4: Ability of the proposed cracking shear strength model to simulate the actual response

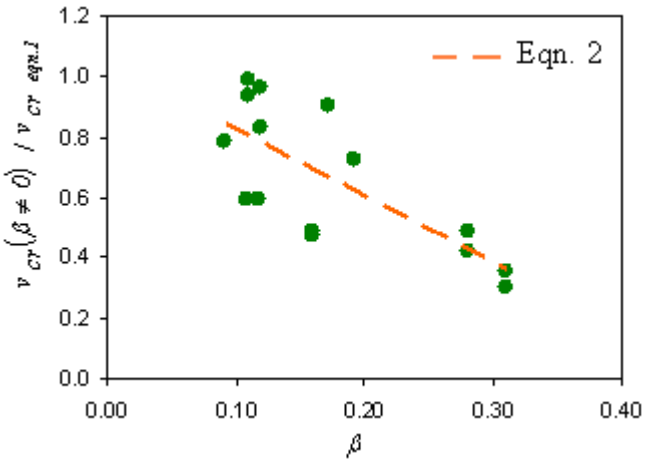

Figure 5: The effect of openings on cracking shear strength of CM walls

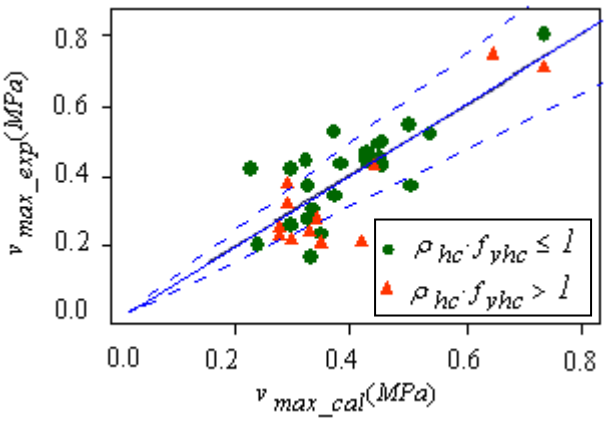

Figure 6: Fitness of the maximum shear model to the experimental data

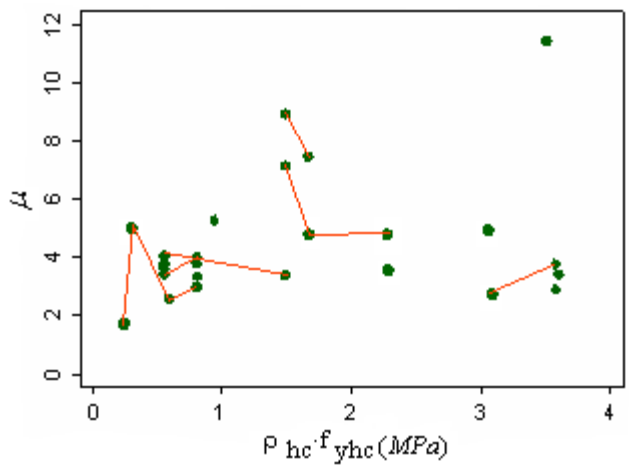

Figure 7: Lack of distinct relationship between μ and $\rho_{hc}.f_{yhc}$ (Specimens with similar characteristics are connected with solid lines)

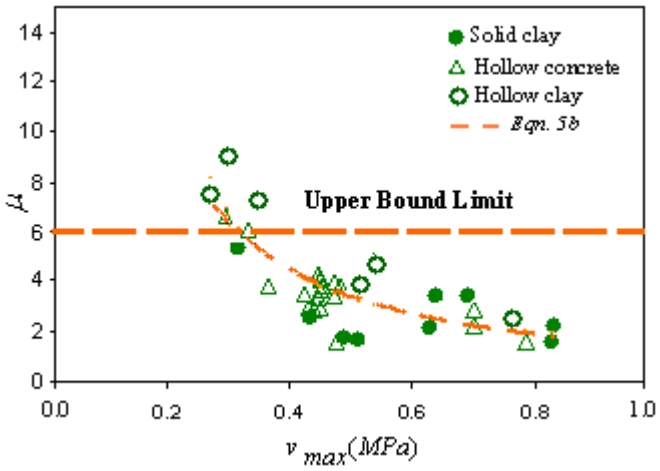

Figure 8: Ability of the proposed equation in predicting the ductility factor

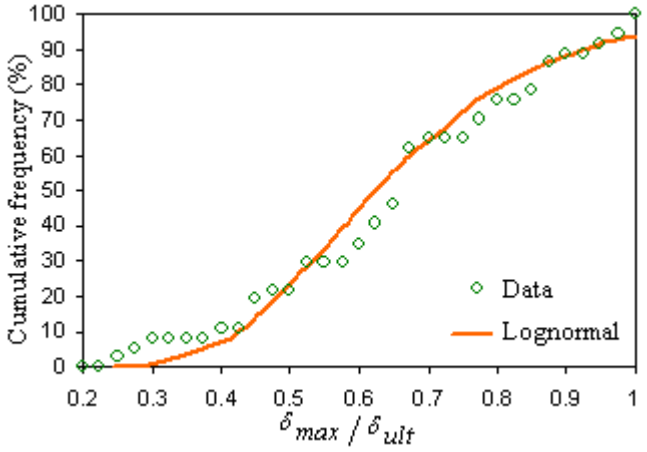

Figure 9: Lognormal distribution of $\delta_{max} / \delta_{ult}$

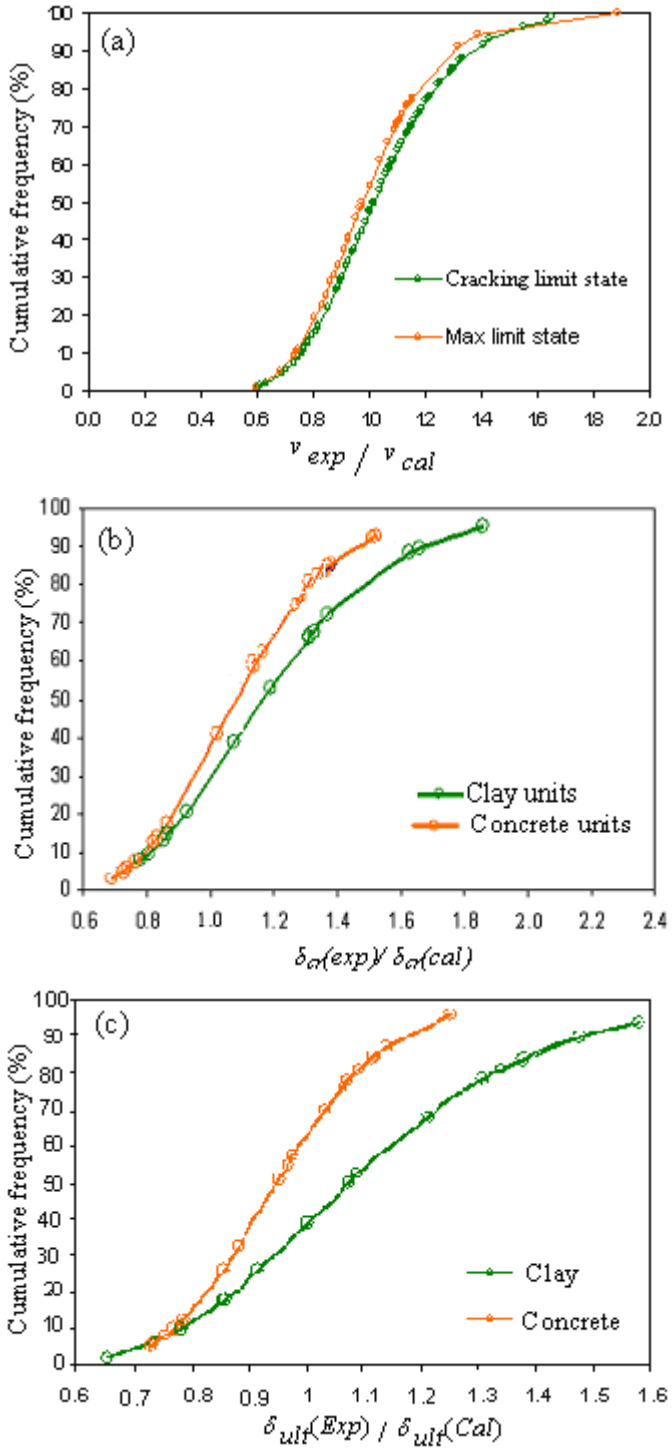

Figure 10: Fragility curves for model parameters at different limit states

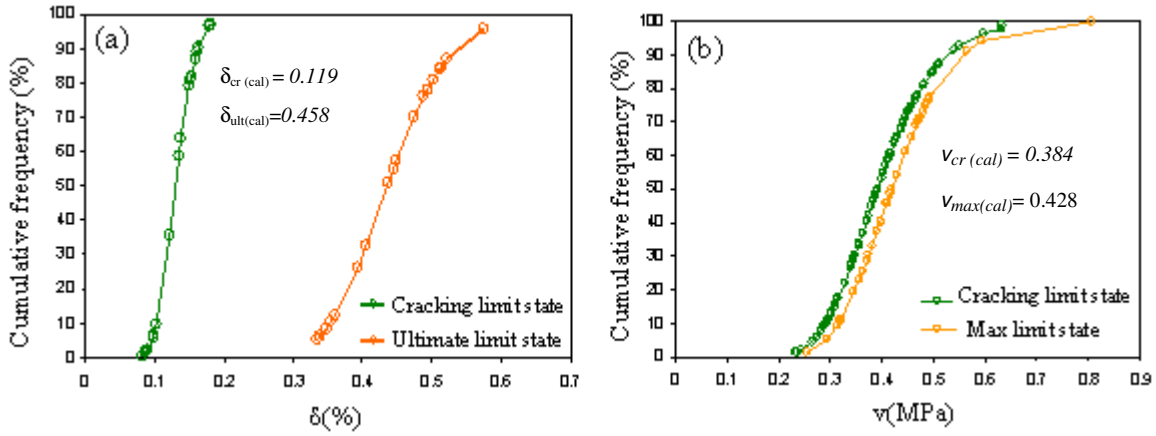

Figure 11: Fragility curves for Specimen 601 from Flores (2004)

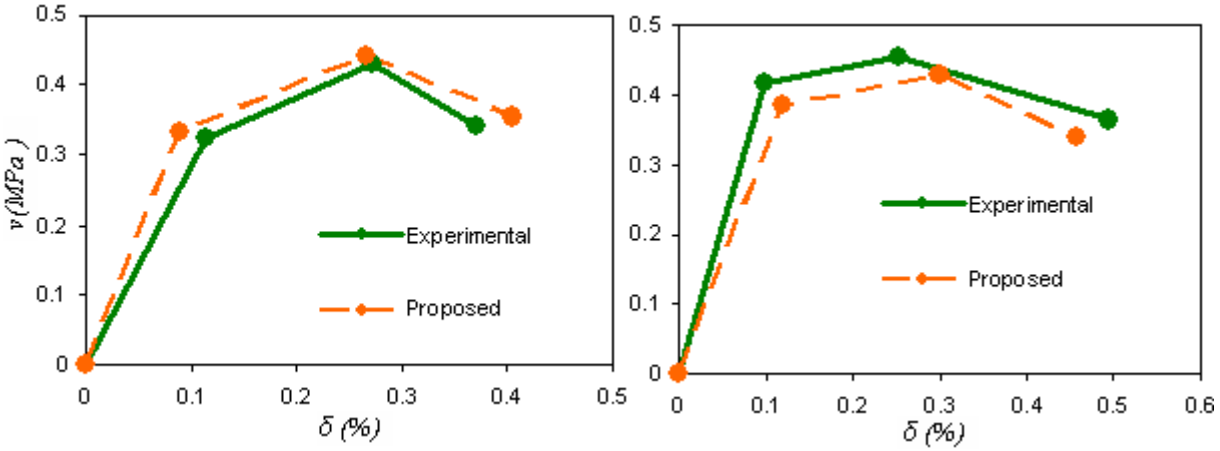

Figure 12: Comparison of experimental and proposed backbones for conforming specimens (a)Marinilli and Castilla, 2006 (Specimen M1); (b) Flores, 2004 (Specimen 601).

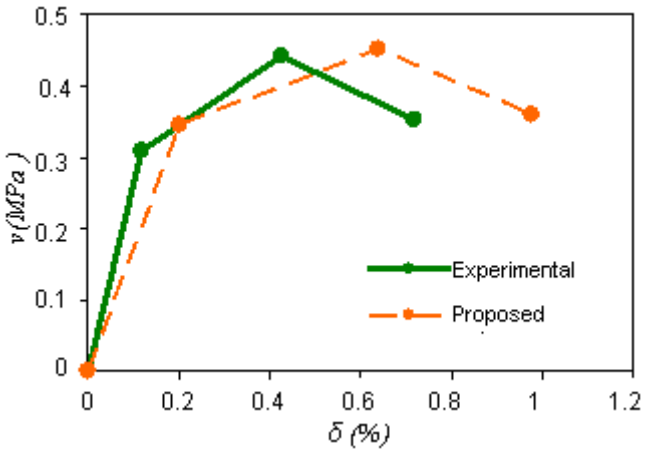

Figure 13: Comparison of experimental and proposed backbones for a CM wall with σ_v/f_m >0.12 (Specimen M-0-E6 from Aguilar et al., 1996)

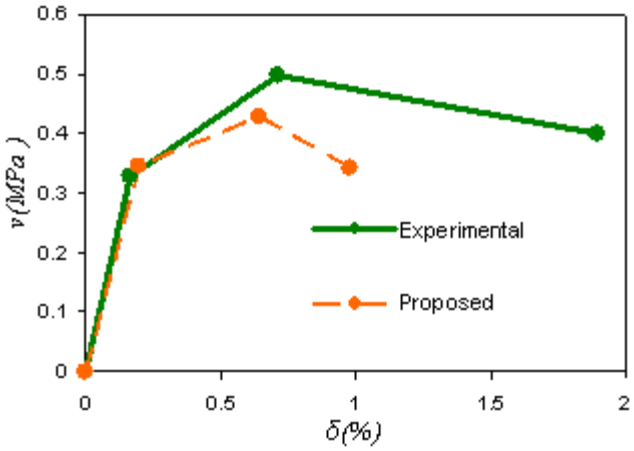

Figure 14: The effect of bed joint reinforcement on the seismic behavior of CM wall (Specimen M-1/4-E6 from Aguilar et al., 1996)